Journal of Materials Chemistry A

ROYAL SOCIETY OF CHEMISTRY

COMMUNICATION

View Article Online
View Journal | View Issue

Cite this: J. Mater. Chem. A, 2022, 10, 13704

Received 1st March 2022
Accepted 31st May 2022

DOI: 10.1039/d2ta01653b

rsc.li/materials-a

Inverse vulcanised sulfur polymer nanoparticles prepared by antisolvent precipitation†

Bowen Zhang, *[a] Samuel Petcher,[a] Romy A. Dop, [a] Peiyao Yan,[a] Wei Zhao,[b] Haoran Wang,[a] Liam J. Dodd,[a] Tom O. McDonald[a] and Tom Hasell *[a]

Elemental sulfur is a by-product of the petrochemicals industry. Some use is found in the production of sulfuric acid and fertilizers, however, supply outstrips demand. Recently, polymers formed from elemental sulfur have been discovered. These 'inverse vulcanised' polymers have a myriad of potential applications including the selective remediation of mercury contaminated wastewater. Herein, we report the synthesis of inverse vulcanised polymer nanoparticles and demonstrate their affinity and selectivity for the removal of mercury from solution. We also demonstrate the generation of an inverse vulcanised membrane for mercury filtration.

Introduction

Sulfur as an element has been known for more than a thousand years.[1] From the first industrial revolution, the worldwide demand for elemental sulfur has soared massively, even leading to the sulfur crisis of 1840.[2,3] However, in the modern world, an excessive supply of elemental sulfur is generated from the petrochemicals industry *via* the hydrodesulfurisation process, in order to decrease the emission of sulfur dioxide in the combustion of fossil fuels, with ~70 million tonnes of elemental sulfur produced annually.[4] Many refining sites have excesses of sulfur stored in stockpiles in open air. Therefore, alternative routes for the use of sulfur have been explored in recent decades, such as for concrete construction and lithium–sulfur batteries.[4,5]

Inverse vulcanisation, reported in 2013, gave a promising approach to use elemental sulfur in large amounts.[6] In this process, a solvent-free system, molten sulfur reacts with small organic molecules, normally divinylic monomers, to generate stable, high sulfur content polymers. The main theoretical mechanisms could be divided in two steps, namely, (1) generation of sulfur diradicals from homolytic cleavage of sulfur rings, and (2) reacting and capping of sulfur diradicals by C=C double bonds. 1,3-diisopropenylbenzene (DIB) was the first crosslinker to be explored in inverse vulcanisation, and the product, poly(S-DIB), was a chemically stable and processable copolymer, which could be used in cathodes for Li–S batteries. Subsequently to this discovery, more economical and more sustainable inverse vulcanisation crosslinkers have been studied in order to maximise the advantage of the low cost and potential sustainability of their combination with sulfur waste, such as limonene,[7] dicyclopentadiene (DCPD),[8] diallyl disulfide,[9–11] divinylbenzenes (DVB),[12] perillyl alcohol (PA),[13] ethylidene norbornene (ENB),[14] and ethylene glycol dimethacrylate (EGDMA).[15,16]

Meanwhile, a variety of corresponding applications, such as IR optics,[4,17,18] Li–S batteries,[4,12,19] construction materials,[4] antimicrobial materials,[20,21] controlled-release fertilisers,[22] adhesives,[11] and mercury capture,[7–9,23–25] were discovered due to these new materials' special properties. In many cases, to achieve a better performance in a given application, the morphology of sulfur polymers was studied as well. To demonstrate their shape-persistency or test their mechanical properties, sulfur polymers are often cured in silicone moulds.[6,8] For Li–S batteries, sulfur polymers are normally ball milled into fine powder.[26] In order to assess the optical properties, such as the transparency in the infrared region, inverse vulcanised polymers are often processed into thin films.[4] There have been even more efforts made in optimising the morphology of sulfur polymers to improve their performance in mercury adsorption. According to Pearson's hard-soft-acid-base (HSAB) principle, sulfur is a "soft" Lewis base and mercury is a "soft" Lewis acid. Thus, it was found sulfur containing polymers had high affinity for mercury. In this application the morphology of inverse vulcanised polymers is crucial because the higher the specific surface area of materials, the larger contacted interface adsorbents can provide to the adsorbates.

[a]Department of Chemistry, University of Liverpool, Crown Street, Liverpool L69 7ZD, UK. E-mail: bowen@liverpool.ac.uk; t.hasell@liverpool.ac.uk
[b]Leverhulme Research Centre for Functional Materials Design, Materials Innovation Factory, University of Liverpool, Crown Street, Liverpool L69 7ZD, UK

† Electronic supplementary information (ESI) available. See https://doi.org/10.1039/d2ta01653b

To this end, typical strategies involve coating polymers onto particles or substrates,[16,24,25,27] electrospinning fibres blended with other polymers,[28] templating by salt,[29] or foaming the inverse vulcanised polymer with supercritical CO_2 to generate porous structures.[30] Almost all of these methods used auxiliary materials to support sulfur polymers and increase their surface area. Additionally, the efficiency of most of these strategies is low, a potential barrier for use on an industrial scale.

Antisolvent precipitation is a versatile method to prepare micro- and nanoparticles, widely used in food and pharmaceutical industries.[31–35] This technique presents several advantages, such as low cost, simple processing, and good potential for scaling up. Reported here for the first time, is the production of sulfur polymer nanoparticles by antisolvent precipitation, yielding nano-materials with high potential for mercury capture.

Results and discussion

Initially, sulfur polymers, poly(Sulfur-Perillyl Alcohol-Dicyclopentadiene) (poly(SPD)), were synthesized through inverse vulcanisation methods (Fig. 1, see ESI† for experimental details). Ternary systems or copolymer blends are commonly used in inverse vulcanisation to increase the reactivity of monomers or adjust the physicochemical properties of final products.[9,36] Additionally, the cost and sustainability of the chemicals were also considered in this synthesis, in which not only elemental sulfur but also DCPD were industrial by-products, and perillyl alcohol is a natural terpene. Fully cured poly(S-dicyclopentadiene) (poly(S-DCPD)) is crosslinked sulfur polymer, which is insoluble in solvents.[8] Poly(S-Perillyl Alcohol) (poly(S-PA)) usually has a low glass transition temperature (T_g) and low molecular weight, preventing shape persistence at ambient temperature. Therefore, SPD was synthesized to generate a soluble sulfur polymer but with higher T_g and molecular weight whilst maintaining solubility. SPD products are denoted as SPD-*X*,*Y*,*Z*, where *X*, *Y*, and *Z* indicate the mass percentage of sulfur, PA, and DCPD, used in the synthesis, respectively. Compared with SPD-50,50,00 (T_g = 31 °C), as shown in Fig. S1,† SPD-50,45,05 and SPD-50,40,10 had higher T_g values, 39 and 47 °C respectively, both of which are above room temperature, resulting from rigid molecular structure and higher potential crosslink density of DCPD.[21] The solubility of the terpolymer decreases significantly as more DCPD, a crosslinker, is added, especially over 30 wt% DCPD (Fig. S2†). SPD-50,45,05 was chosen to study further as this gave a sufficient increase to M_w and T_g, while still maintaining high solubility. 500 mg of SPD-50,45,05 (solute) was initially dissolved in 10 mL of chloroform ($CHCl_3$) (solvent) to generate a 50 mg mL^{-1} polymer solution. 10 μL, 50 μL, 100 μL, and 250 μL of solution was added to 10 mL ethanol (anti-solvent) dropwise with stirring (500 rpm) at room temperature to precipitate nanoparticles (solubility study shown in Table S1†). No surfactant was involved in the synthesis to keep the processing facile and to avoid contaminating the surface of nanoparticles, which will be used as sorbents for heavy metals. Samples were denoted as SPD-50,45,05-*A*, where *A* is the volume of polymer solution in microlitres. From Dynamic Light Scattering (DLS) results, as shown in Fig. 2a, it can be found that sulfur nanoparticles were successfully prepared with *z*-average diameter from ~100 nm to 1000 nm. The correlograms of these particles (Fig. S3 and S4†) show a smooth decay as expected for particles of this size range which are suitable for analysis by DLS. As more polymer solution was added, a second size range, from ~2000 nm to 3500 nm, can be observed. The increase in average hydrodynamic diameter of these particles with increasing polymer content is evident from a slightly slower decay in the correlation function (Fig. S5 and S6†). SPD-50,45,05-10 formed the most uniform nanoparticles, which have narrow size distributions (polydispersity index, PDI, 23%), with hydrodynamic diameter of 486 nm. As the solvent to anti-solvent ratio increased, the distribution of particle size became much broader, and the hydrodynamic diameter increased to 590 nm in the case of SPD-50,45,05-50, indicating an increase in particle size as well. This result aligned with reported studies that particle size can be reduced by increasing the anti-solvent-to-solvent ratio.[31] For SPD-50,45,05-100 and SPD-50,45,05-250, both distributions were broader and aggregation was more prevalent. The morphology of nanoparticles prepared under different conditions was observed through scanning electron microscopy (SEM). Similar to the conclusion from DLS testing, it could be found that the shape of SPD-50,45,05-10 (Fig. 2b and c and S7†) is more uniform than others (Fig. 2d and S8 and S9†), although all particles analysed by SEM appeared smaller size than that shown in DLS, which is to be expected as DLS measures the hydrodynamic radius while SEM images are obtained on the dried particles. SEM images also revealed that the shape of SPD-50,45,05-10 is more uniform and spherical than that of SPD-50,45,05-250, which had other irregular shapes, such as elongated spheroids and aggregates. However, considering that the application of sulfur polymer nanoparticles is to uptake mercury, non-uniform shapes and aggregation are likely acceptable as their increased surface area to volume ratio might increase the productivity. Additionally, large diameters are also preferred as the larger size of the particles assists retrieval of the

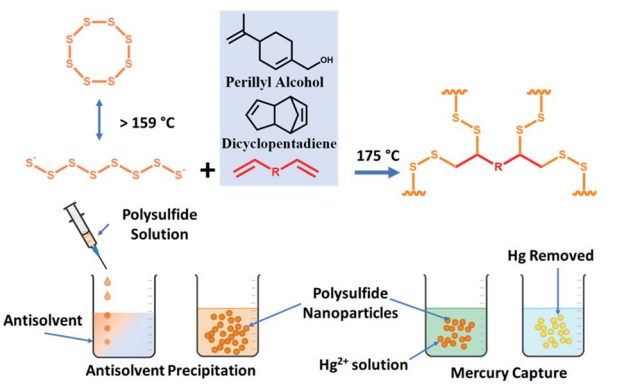

Fig. 1 (a) Schematic for general inverse vulcanisation, and cross-linkers, *e.g.* DCPD and perillyl alcohol. (b) Schematic for antisolvent precipitation and application of polysulfide nanoparticles in mercury capture.

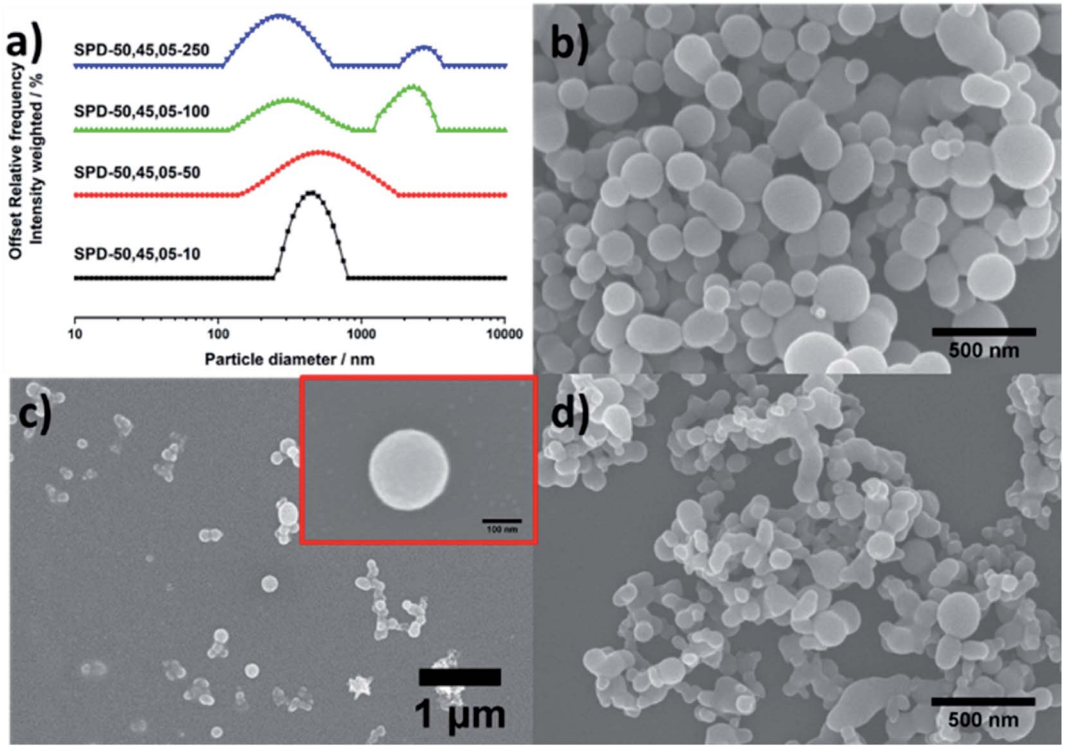

Fig. 2 (a) Size distribution of polysulfide nanoparticles characterised by DLS. (b and c) SEM image of SPD-50,45,05-10, showing polysulfide nanoparticles mostly uniform and spherical, as the example shown in (c). (d) SEM image of SPD-50,45,05-250, indicating although nanoparticles formed through antisolvent precipitation, the shape of particles are irregular and not uniform.

particles by sedimentation, filtration, or, centrifugation. Therefore SPD-50,45,05-250 was selected as a representative sample for further characterisation and application test.

From ^{1}H NMR spectroscopy of SPD-50,45,05, as shown in Fig. 3a, it could be found that C=C double bonds of both perillyl alcohol (vinylic protons: from 4.0 ppm to 4.7 ppm) and DCPD (vinylic protons: from 5.5 ppm to 5.9 ppm) were fully reacted. The broad peaks from 3.6 to 3.7 ppm were assigned as the protons on the generated S–C–H, further confirming the reaction of sulfur and C=C double. Compared with SPD-50,45,05, SPD-50,45,05-250 has negligible differences in ^{1}H NMR spectroscopy, indicating the chemical structure of polymer has no obvious change

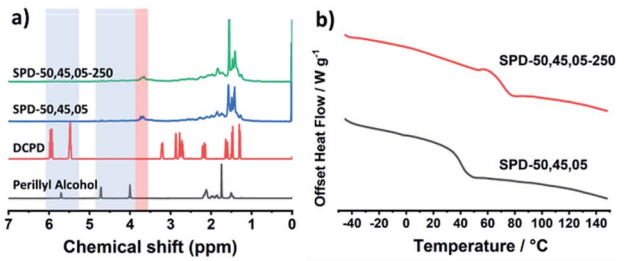

Fig. 3 (a) ^{1}H NMR spectra of polysulfide nanoparticles, SPD-50,45,05-250, and bulk polysulfide, SPD-50,45,05 dissolved in $CDCl_3$. Vinylic protons of DCPD and perillyl alcohol were assigned and highlighted by blue band. The new generated peaks, highlighted by red band, are assigned as H–C–S positions (b) offset DSC traces for polysulfide nanoparticles, SPD-50,45,05-250, and bulk polysulfide SPD-50,45,05.

before and after antisolvent precipitation. Elemental analysis for both SPD-50,45,05 and SPD-50,45,05-250 was been performed, showing a slight difference before and after treatment, as shown in Table S2.† This may be because the dissolution of the polymer extracts lower molecular weight polymers which then do not precipitate when added to the anti-solvent, thus shifting the elemental composition. In the comparison of DSC results, as shown in Fig. 3b, it can be found that nanoparticles, SPD-50,45,05-250, have higher T_g = 63 °C than that (T_g = 33 °C) of bulk materials, SPD-50,45,05. Similar results that nanoparticles had higher T_g than their corresponding precursors are observed in other samples (Fig. S10 and S11†). The reason for these results were speculated to be that small molecules and oligomers, acting as a plasticiser and suppressing the T_g in the pristine polymer, could be dissolved in antisolvent and washed out, leaving only relatively high molecular weight polymers to generate nanoparticles. This speculation was further supported by GPC results, as shown in Fig. S12;† the M_n and M_w of SPD-50,45,05 was 455 and 1242, respectively, and M_n/M_w = 2.734, while after antisolvent precipitation, M_n and M_w of SPD-50,45,05-250 was 669 and 1281, respectively, and M_n/M_w = 1.916. Similar results were achieved from GPC results of SPD-50,50,00 (M_n = 608 and M_w = 809, M_n/M_w = 1.33)/SPD-50,50,00-250 (M_n = 724 and M_w = 907, M_n/M_w = 1.25) and SPD-50,40,10 (M_n = 713 and M_w = 2676, M_n/M_w = 3.76)/SPD-50,40,10-250 (M_n = 1207 and M_w = 2906, M_n/M_w = 2.407). These indicate that increasing the ratio of DCPD increased the molecular weight of poly(SPD), aligning with the results from DSC testing, and that the average molecular weight

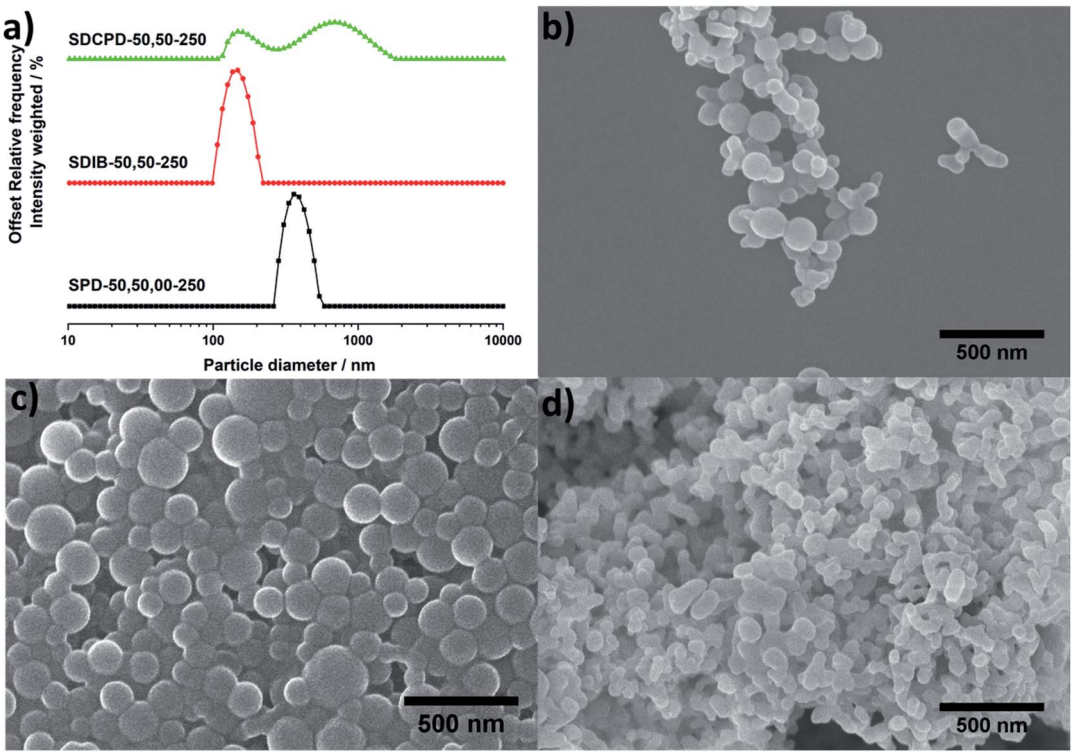

Fig. 4 (a) Size distribution of polysulfide nanoparticles characterised by DLS. (b) SEM image of SPD-50,50,00-250. c) SEM image of SDIB-50,50-250. d) SEM image of SDCPD-50,50-250.

of all poly(SPD) increased and the distribution became more uniform, post antisolvent precipitation. Higher molecular weights and T_g values may make it possible for the sulfur polymer nanoparticles to be applied as mercury sorbents at room temperature, owing to the increased hardness and shape persistency. By the same method as before, other inverse vulcanised polymers, such as poly (sulfur-diisopropenyl benzene) (poly(S-DIB)), poly(S-PA), and partly cured poly(S-DCPD), were synthesized into nanoparticles, SDIB-50,50-250, SPD-50,50,00-250, and SDCPD-50,50-250, correspondingly, as shown in Fig. 4 and the DLS correlograms can be seen in Fig. S13–S15.† From both DLS (Fig. 4a) and SEM results (Fig. 4c), it could be found that SDIB-50,50-250 had the most uniform size (PDI, 7.3%) and spherical shape, and the smallest particle diameters (hydrodynamic diameter, 167 nm). However, nanoparticles at this size are not easily collected by filtration, compared to larger particles. The morphologies of SDCPD-50,50-250 and SPD-50,50,00-250 were very similar, containing both spheres and other irregular shapes. However, SDCPD-50,50-250 showed large amounts of aggregation, which speculatively is due to the same reason for the observed aggregation in SPD-50,45,05-250. Therefore, it can be concluded that the morphology of sulfur polymer nanoparticles is highly depended on the precursors, and the solvent–antisolvent system. Owing to relatively large particle sizes and aggregation, simple prototypes of mercury filter membranes could be prepared from sulfur polymer nanoparticles, by supporting them on commercial 0.20 μm PTFE membranes and 0.45 μm nylon syringe filters, as shown in Fig. 5 and S16.†

Mercury pollution is an urgent global health concern which has led to more than 120 countries signing a joint agreement to reduce mercury emissions.[29,37,38] Elemental sulfur, metal sulfides, and polysulfides are commonly used as mercury sorbents, because of the interaction between a “soft” Lewis base, sulfur; and a “soft” Lewis acid, mercury. Mercury uptake also benefits from porosity and high specific surface area. Therefore, various structures and shapes of polysulfides were exploited by different research groups. Nano-sized polysulfides demonstrated good performance and high efficiency in mercury capture, however, previously reported sulfur containing nanomaterials required other auxiliary materials, such as a porogen or support materials.[16,24,28–30] SPD-50,45,05-250, as well as other

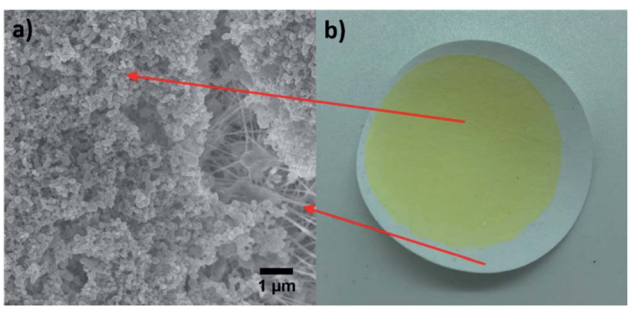

Fig. 5 (a) SEM image of polysulfide nanoparticles supported on the commercial 0.20 μm PTEF membrane, showing polysulfide nanoparticles and PTFE nanofibres. (b) Prototype membrane supported sulfur polymer for mercury removal.

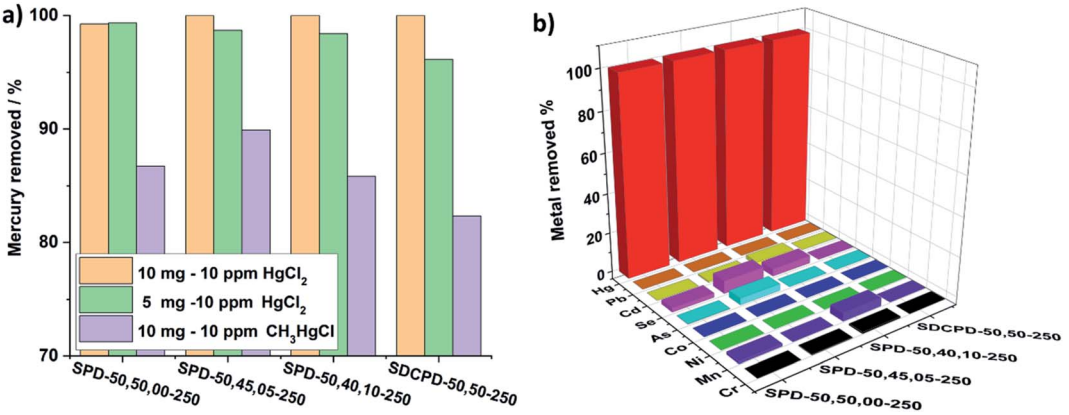

Fig. 6 (a) Static mercury uptake test of various polysulfide nanoparticles with $HgCl_2$ and CH_3HgCl. (b) Selectivity test of polysulfide nanoparticles using mixed ion solution, simulating waste water. Mercury could be removed totally and selectively. Concentration of specific ions in the CRM is: Cr, 331 ppb, Mn, 1134 ppb, Ni 1215, ppb, Co, 876 ppb, As, 248 ppb, Se, 129 ppb, Cd, 434 ppb, Hg, 9.7 ppb, Pb, 243 ppb.

nanoparticles were tested as mercury sorbents for aqueous solutions. Initially, the required mass of nanoparticles was weighed into a centrifuge tube, followed by dispensing of 10 mL of aqueous $HgCl_2$ solution of a required concentration. From the results, as shown in Fig. 6a and Table S3,† almost all aqueous mercury was removed from a 10 ppm $HgCl_2$ solution by using 10 mg polysulfide nanoparticles, and more than 95% of mercury was removed from 10 ppm $HgCl_2$ solution by using 5 mg polysulfide nanoparticles. Additionally, polysulfide nanoparticles were also applied in capturing methylmercury chloride from aqueous solution. From Fig. 6a and Table S3,† it could be found that the removal of methylmercury chloride is not as effective as $HgCl_2$, however, all polysulfide nanoparticles could uptake more than 80% mercury from 10 ppm aqueous solution. These results are performed better than commercial mercury adsorbent, activated carbons, in similar initial concentration mercury solution (as shown in Table S4†).[39,40] More specifically, in comparison with bulk polysulfide materials in same components (Table S4†), polysulfide nanoparticles were demonstrated significant improvement in mercury uptake. Taking poly(S-DCPD) as an example, the mercury capacity of SDCPD-50,50-250 in static testing ($C_0 = 10$ ppm) has reached to 19.1 mg g^{-1}, much higher than that of S-DCPD (0.1 mg g^{-1}, $C_0 =$ 2 ppm),[8] saturation capacity of salt templated of S-DCPD (2.27 mg g^{-1}),[29] and saturation capacity of S-DCPD coated silica gel (5 mg g^{-1}).[27] Similarly, SPD-50,50,00-250 has much higher mercury capacity (19.5 mg g^{-1}, $C_0 = 10$ ppm) than its counterpart bulk materials (0.05 mg g^{-1}, $C_0 = 2.5$ ppm).[13] Not only performed better than same component bulk polysulfide, in mercury uptake application, these novel nanoparticles were also comparable to other polysulfides synthesized by other crosslinkers, such as poly (S-*r*-canola) (1.81 mg g^{-1}),[38] poly (S-*r*-rice bran) (1.92 mg g^{-1}),[38] poly(S-*r*-castor) (2.01 mg g^{-1}),[38] and poly(sulfur-GOB-DCPD) (1.60 mg g^{-1} $C_0 = 20$ ppm).[9] Admittedly, some inversed vulcanised polymer were reported with higher mercury uptake capacity than that of nanoparticles,[16,28] the relatively simple preparation processing (with no auxiliary materials) and higher productivity were significant advantages of inverse vulcanised polymer nanoparticles. Finally, the efficiency of the sorbent to remove mercury in more realistic conditions was studied.[41] Naturally, mercury concentration in groundwater and surface water is less than 0.5 ppb, however, it could be up to 5.5 ppb in volcanically active locations. According to an exposure study, the World Health Organisation (WHO) suggested that 6 ppb of inorganic mercury in daily drinking water is a maximum guideline value for an adult. Therefore, lower mercury concentration solutions with competing metal ions were applied to simulate contaminated waste water. All sulfur polymer nanoparticles were demonstrated to have high efficiency and high selectivity for mercury removal, as all mercury (9.70 ppb, 10 mL) was selectively removed from mixed metal ion solutions in 1 hour, as shown in Fig. 6b and Table S5.† Finally, the mercury filter prototype produced by SPD-50,45,05-250 supported on commercial PTFE membrane filter, was tested upon a mixed ion solution. Compared with a blank membrane filter, which reduced the original mercury concentration from 7.52 ppb to 7.15 ppb, the mercury filter prototype performed with high efficiency and high selectivity for instantaneous filtration of mercury, which removed almost 90% of the mercury, 7.52 ppb to 0.78 ppb (average of three tests), a result more relevant in industry applicable conditions (shown in Fig. S17 and Table S6†).

Conclusions

In conclusion, we have explored an antisolvent precipitation method to produce nanoparticles of inverse vulcanised polymer. The resultant polysulfide nanoparticles are simple to prepare and have good potential for scaling up. Benefiting from nano-structure and high sulfur content, polysulfide nanoparticles could be applied as highly selective sorbents in mercury removal from extremely low mercury concentration (ppb level) to high mercury concentration (ppm level). Moreover, these polysulfide nanoparticles are also demonstrated as effective mercury filter membranes. Finally, the applicability of these polysulfide nanoparticles is not limited to mercury

removal and water purification; they may also be potentially applied in Li–S batteries and catalysts.

Author contributions

Bowen Zhang: conceptualization, methodology, investigation, formal analysis, writing–original draft, writing–review & editing. Samuel Petcher: investigation, formal analysis, writing–review & editing. Romy A. Dop: investigation. Peiyao Yan: investigation. Wei Zhao: investigation. Haoran Wang: investigation. Liam J Dodd: investigation. Tom O. McDonald: formal analysis, writing–review & editing. Tom Hasell: resources, writing–review & editing, supervision, project administration, funding acquisition.

Conflicts of interest

There are no conflicts to declare.

Acknowledgements

T. H. holds a Royal Society University Research Fellowship.

Notes and references

1 M. Schmidt, in *New Uses of Sulfur*, 1978, pp. 1–12.
2 M. Šedivý, *J. Mod. Ital. Stud.*, 2011, **16**, 1–18.
3 D. W. Thomson, *Eur. Hist. Q.*, 1995, **25**, 163–180.
4 J. J. Griebel, R. S. Glass, K. Char and J. Pyun, *Prog. Polym. Sci.*, 2016, **58**, 90–125.
5 M. J. H. Worthington, R. L. Kucera and J. M. Chalker, *Green Chem.*, 2017, **19**, 2748–2761.
6 W. J. Chung, J. J. Griebel, E. T. Kim, H. Yoon, A. G. Simmonds, H. J. Ji, P. T. Dirlam, R. S. Glass, J. J. Wie, N. A. Nguyen, B. W. Guralnick, J. Park, Á. Somogyi, P. Theato, M. E. Mackay, Y. Sung, K. Char and J. Pyun, *Nat. Chem.*, 2013, **5**, 518–524.
7 M. P. Crockett, A. M. Evans, M. J. H. Worthington, I. S. Albuquerque, A. D. Slattery, C. T. Gibson, J. A. Campbell, D. A. Lewis, G. J. L. Bernardes and J. M. Chalker, *Angew. Chem., Int. Ed.*, 2016, **55**, 1714–1718.
8 D. J. Parker, H. A. Jones, S. Petcher, L. Cervini, J. M. Griffin, R. Akhtar and T. Hasell, *J. Mater. Chem. A*, 2017, **5**, 11682–11692.
9 B. Zhang, L. J. Dodd, P. Yan and T. Hasell, *React. Funct. Polym.*, 2021, **161**, 104865.
10 I. Gomez, O. Leonet, J. A. Blazquez and D. Mecerreyes, *ChemSusChem*, 2016, **9**, 3419–3425.
11 C. Herrera, K. J. Ysinga and C. L. Jenkins, *ACS Appl. Mater. Interfaces*, 2019, **11**, 35312–35318.
12 M. Arslan, B. Kiskan, E. C. Cengiz, R. Demir-Cakan and Y. Yagci, *Eur. Polym. J.*, 2016, **80**, 70–77.
13 D. J. Parker, S. T. Chong and T. Hasell, *RSC Adv.*, 2018, **8**, 27892–27899.
14 J. A. Smith, X. Wu, N. G. Berry and T. Hasell, *J. Polym. Sci., Part A: Polym. Chem.*, 2018, **56**, 1777–1781.
15 B. Zhang, H. Gao, P. Yan, S. Petcher and T. Hasell, *Mater. Chem. Front.*, 2020, **4**, 669–675.
16 X. Wu, J. A. Smith, S. Petcher, B. Zhang, D. J. Parker, J. M. Griffin and T. Hasell, *Nat. Commun.*, 2019, **10**, 647.
17 D. A. Boyd, V. Q. Nguyen, C. C. McClain, F. H. Kung, C. C. Baker, J. D. Myers, M. P. Hunt, W. Kim and J. S. Sanghera, *ACS Macro Lett.*, 2019, **8**, 113–116.
18 J. Kuwabara, K. Oi, M. M. Watanabe, T. Fukuda and T. Kanbara, *ACS Appl. Polym. Mater.*, 2020, **2**, 5173–5178.
19 O. Bayram, B. Kiskan, E. Demir, R. Demir-Cakan and Y. Yagci, *ACS Sustainable Chem. Eng.*, 2020, **8**, 9145–9155.
20 J. A. Smith, R. Mulhall, S. Goodman, G. Fleming, H. Allison, R. Raval and T. Hasell, *ACS Omega*, 2020, **5**, 5229–5234.
21 R. A. Dop, D. R. Neill and T. Hasell, *Biomacromolecules*, 2021, **22**, 5223–5233.
22 M. Mann, J. E. Kruger, F. Andari, J. McErlean, J. R. Gascooke, J. A. Smith, M. J. H. Worthington, C. C. C. McKinley, J. A. Campbell, D. A. Lewis, T. Hasell, M. V. Perkins and J. M. Chalker, *Org. Biomol. Chem.*, 2019, **17**, 1929–1936.
23 S. Petcher, B. Zhang and T. Hasell, *Chem. Commun.*, 2021, **57**, 5059–5062.
24 J. M. Scheiger, C. Direksilp, P. Falkenstein, A. Welle, M. Koenig, S. Heissler, J. Matysik, P. A. Levkin and P. Theato, *Angew. Chem., Int. Ed.*, 2020, **59**, 18639–18645.
25 L. A. Limjuco, H. T. Fissaha, H. Kim, G. M. Nisola and W. J. Chung, *ACS Appl. Polym. Mater.*, 2020, **2**, 4677–4689.
26 A. G. Simmonds, J. J. Griebel, J. Park, K. R. Kim, W. J. Chung, V. P. Oleshko, J. Kim, E. T. Kim, R. S. Glass, C. L. Soles, Y. E. Sung, K. Char and J. Pyun, *ACS Macro Lett.*, 2014, **3**, 229–232.
27 M. Mann, B. Zhang, S. J. Tonkin, C. T. Gibson, Z. Jia, T. Hasell and J. M. Chalker, *Polym. Chem.*, 2022, **13**, 1320–1327.
28 M. Thielke, L. Bultema, D. Brauer, B. Richter, M. Fischer and P. Theato, *Polymers*, 2016, **8**, 266.
29 S. Petcher, D. J. Parker and T. Hasell, *Environ. Sci.: Water Res. Technol.*, 2019, **5**, 2142–2149.
30 T. Hasell, D. J. Parker, H. A. Jones, T. McAllister and S. M. Howdle, *Chem. Commun.*, 2016, **52**, 5383–5386.
31 I. J. Joye and D. J. McClements, *Trends Food Sci. Technol.*, 2013, **34**, 109–123.
32 M. E. Matteucci, M. A. Hotze, K. P. Johnston and R. O. Williams, *Langmuir*, 2006, **22**, 8951–8959.
33 C. Hogarth, K. Arnold, A. McLauchlin, S. P. Rannard, M. Siccardi and T. O. McDonald, *J. Mater. Chem. B*, 2021, **9**, 9874–9884.
34 J. M. Taylor, K. Scale, S. Arrowsmith, A. Sharp, S. Flynn, S. Rannard and T. O. McDonald, *Nanoscale Adv.*, 2020, **2**, 5572–5577.
35 T. O. McDonald, L. M. Tatham, F. Y. Southworth, M. Giardiello, P. Martin, N. J. Liptrott, A. Owen and S. P. Rannard, *J. Mater. Chem. B*, 2013, **1**, 4455–4465.
36 J. A. Smith, S. J. Green, S. Petcher, D. J. Parker, B. Zhang, M. J. H. Worthington, X. Wu, C. A. Kelly, T. Baker, C. T. Gibson, J. A. Campbell, D. A. Lewis, M. J. Jenkins, H. Willcock, J. M. Chalker and T. Hasell, *Chem.–Eur. J.*, 2019, 10433–10440.

37 M. Mann, X. Luo, A. Tikoalu, C. T. Gibson, Y. Yin, R. Al-attabi, G. G. Andersson, C. L. Raston, L. C. Henderson, A. Pring, T. Hasell and J. M. Chalker, *Chem. Commun.*, 2021, **57**, 6296–6299.
38 A. D. Tikoalu, N. A. Lundquist and J. M. Chalker, *Adv. Sustainable Syst.*, 2020, **4**, 1–9.
39 C. Liu, J. Peng, L. Zhang, S. Wang, S. Ju and C. Liu, *J. Cleaner Prod.*, 2018, **196**, 109–121.
40 J. S. M. Lee, D. J. Parker, A. I. Cooper and T. Hasell, *J. Mater. Chem. A*, 2017, **5**, 18603–18609.
41 W. H. O. WHO, WHO, 2005, WHO/SDE/WS, WHO/SDE/WSH/05.08/10.

